

Single particle transfer reactions and backward angle elastic scattering for the ^{15}N , $^{16}\text{O} + ^{28}\text{Si}$ systems

S. Kahana

Brookhaven National Laboratory, Upton, New York 11973

B. T. Kim and M. Mermaz

Departement de Physique Nucleaire, Centre d'Etudes Nucleaires de Saclay, 91190 Gif-sur-Yvette, France

(Received 21 June 1979)

Strongly absorbing optical potentials in a distorted-wave context are unable to describe the single neutron-stripping and single proton-pickup reactions induced by 44 MeV ^{15}N on a ^{28}Si target. Modifications of the imaginary potential consistent with the surface transparency requirements for backward angle $^{16}\text{O} + ^{28}\text{Si}$ elastic scattering greatly improve the transfer predictions. In addition, the altered potentials yield a reasonably qualitative picture of the backward elastic excitation function over a broad range of energy.

[NUCLEAR REACTIONS $^{28}\text{Si}(^{15}\text{N}, ^{16}\text{O})$, $^{28}\text{Si}(^{15}\text{N}, ^{14}\text{N})$, excitation function and angular distribution for elastic scattering.]

I. INTRODUCTION

A recent paper¹ describing the $^{28}\text{Si}(^{15}\text{N}, ^{16}\text{O})$ and $^{28}\text{Si}(^{15}\text{N}, ^{14}\text{N})$ reactions at a laboratory energy $E_{\text{lab}} = 44$ MeV indicated that some difficulties occur in distorted-wave Born approximation (DWBA) or coupled-channel Born approximation (CCBA) attempts to fit the measured differential cross sections to strongly excited single particle states in the final ^{27}Al and ^{29}Si nuclei. The discrepancies between distorted-wave calculations and experiment, especially severe for transitions to the $\frac{5}{2}^+$ ground state and $\frac{1}{2}^+$ 0.84 MeV excited states in ^{27}Al , occur despite the use of optical potentials carefully fitted to the $^{15}\text{N} + ^{28}\text{Si}$, $E_{\text{lab}} = 44$ MeV, $^{16}\text{O} + ^{27}\text{Al}$, $E_{\text{lab}} = 46.49$ MeV, and $^{14}\text{N} + ^{28}\text{Si}$, $E_{\text{lab}} = 38.98$ MeV data. These potentials, whose optical parametrizations¹ are listed in Table I, may be considered to be of the strong absorption variety, possessing an appreciable imaginary part in the grazing region between ions so crucial to the single particle transfer reactions. Specifically, the theoretical problems occurring are a major failure to fit the observed angular distributions and absolute cross-section magnitudes in the proton-pickup reactions, and a more minor inability of the DWBA or CCBA to fit the more forward

angular differential cross section in the neutron-stripping reaction. The observed ($^{15}\text{N}, ^{16}\text{O}$) angular distributions for transitions to the $\frac{5}{2}^+$ ground state and 0.84 $\frac{1}{2}^+$ excited ^{27}Al states (see dashed curves in Fig. 2) are oscillatory and forward rising, while the calculations, using the potentials in Table I, are bell shaped. Very similar results are obtained by use of folded potentials¹ which possess identical imaginary and real geometry. The folded potential chosen in this fashion may also be considered strongly absorbing in the grazing region. In addition, these calculations using strong absorption underpredict the cross-section magnitudes near the grazing angles ($\sim 30^\circ$) by approximately a factor of 2–3, and at forward angles by an order of magnitude. CCBA calculations do not seem to improve the DWBA results, yielding small effects for transitions to what are considered strong single particle states. We will, in fact, limit our discussion in this work to such states.

II. ANALYSIS USING SURFACE TRANSPARENT OPTICAL POTENTIALS

The purpose of this note is to demonstrate that minor changes in the absorptive parts of the op-

TABLE I. Strong absorbing optical potentials from Mermaz *et al.* (Ref. 10). Standard Woods-Saxon volume forms are used for the real and imaginary potentials.

System	E_{lab}	V	r_v	a_v	W_v	r_I	a_I	Family
$^{15}\text{N} + ^{28}\text{Si}$	44.0	30	1.168	0.689	19.20	1.168	0.689	OMP 1 IN
$^{16}\text{O} + ^{27}\text{Al}$	46.5	30	1.120	0.713	24.76	1.120	0.713	OMP 1 OUT
$^{14}\text{N} + ^{28}\text{Si}$	39.0	30	1.089	0.764	29.91	1.089	0.764	OMP 1 OUT

TABLE II. Surface-transparent optical potentials. Volume Woods-Saxon forms are used for the real and imaginary potentials, but an additional surface derivative—Woods-Saxon is added to the imaginary potential. Thus, the imaginary potential reads

$$W(r) = -W_v f[x(r_v, R_v, a_v)] + 4W_s f' [x(r, R_s, a_s)]$$

with

$$f(x) = [1 + \exp(x)]^{-1} \text{ and } x = (r - R)/a$$

and

$$R_i = r_i (A_1^{1/3} + A_2^{1/3}) \text{ etc. } i = v, s.$$

The potentials ST differ from OMP in having a volume absorptive part with a greatly reduced diffusivity and a slightly reduced imaginary radius.

System	V	r_v	a_v	W_v	r_I	a_I	W_s	Family
$^{15}\text{N} + ^{28}\text{Si}$	30	1.168	0.689	30	1.0	0.2	3.0	ST 1
$^{16}\text{O} + ^{27}\text{Al}$	30	1.120	0.713	30	1.0	0.2	1.5	ST 2
$^{14}\text{N} + ^{29}\text{Si}$	30	1.089	0.764	30	1.0	0.2	5.0	ST 3
			$a_s = a_v$		$r_s = r_v$			

tical potentials can simultaneously correct all of the predictive faults. These minor changes, however, do produce a qualitatively different absorption, rendering the optical potentials in Table I surface transparent and somewhat more volume opaque. Such volume-opaque surface-transparent potentials have arisen much earlier in connection with forward hemisphere quasielastic reactions² and certainly the surface transparency seems absolutely necessary for optical descriptions of the recently observed backward angle elastic scattering in $^{16}\text{O} + ^{28}\text{Si}$, $^{12}\text{C} + ^{28}\text{Si}$ systems.³⁻⁶ Table II contains a list of the potential parameters used in this note for the single entrance and two exit channels. The major difference between the potentials described by Tables I and II is the addition for Table II of a small surface peaked absorptive part and the use of a volume absorptive part with a greatly reduced diffusivity $a_I = 0.2-0.3$ fm and a slightly reduced imaginary radius $r_I = 1.0$ fm.

The fits to elastic data obtained from surface transparent (ST) potentials are displayed in Fig. 1. Fits from optical model potentials (OMP) essentially pass through all experimental points. Clearly some slight oscillations are produced theoretically with ST potentials for the most backward angles measured at the Saclay Tandem Van de Graaff Facility but are not excluded by the present data. In any case, small compensatory changes in the real potentials in Table II could produce more exact fitting; also elastic data taken in the backward hemisphere would clearly be of great value. At the most backward angles the $^{15}\text{N} + ^{28}\text{Si}$ and $^{16}\text{O} + ^{27}\text{Al}$ calculated elastic cross sections exhibit the characteristic behavior observed in the $^{16}\text{O} + ^{28}\text{Si}$ system, but with a reduced magnitude. The value of $(\sigma_{\text{elastic}}/\sigma_{\text{Rutherford}})$ (180°) for

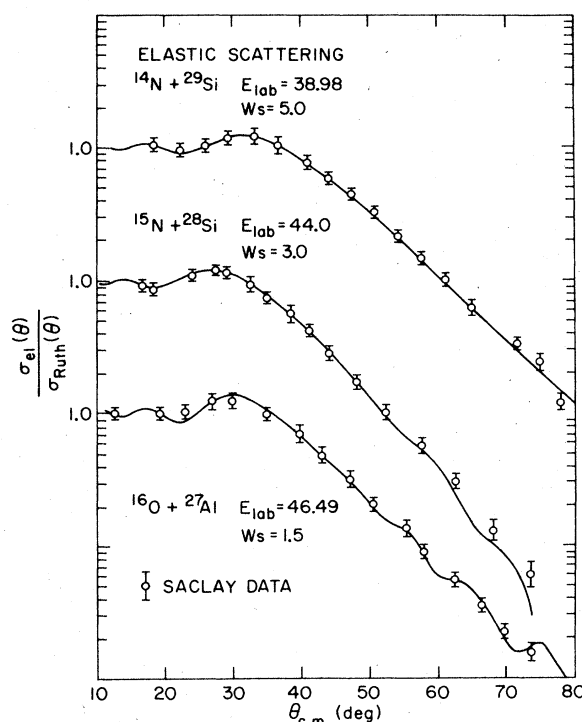


FIG. 1. Elastic scattering for the entrance and exit channels of the direct reactions discussed in this work. The theoretical calculations are those obtained using the appropriate potential ST 1, 2, 3 in Table II, i.e., using surface-transparent volume-opaque potentials. No attempt was made to achieve a fit. The OMP's in Table II, adjusted as described in the text, yielded the results of this figure. The key parameter in determining the more backward angle elastic scattering, the surface absorption W_s , could be increased for $^{15}\text{N} + ^{28}\text{Si}$ with some improvement in the elastic scattering and no deterioration in the transfer results. The values $W_s = 5.0, 3.0, 1.5$ MeV represent reasonable choices, not fitted values.

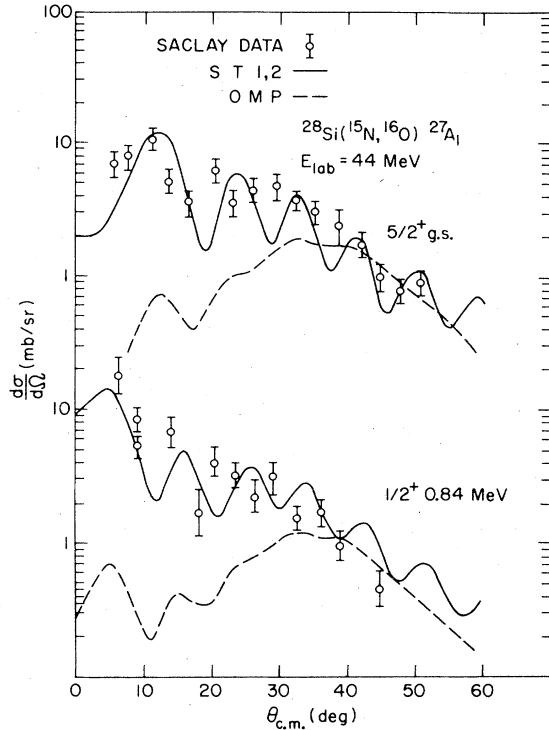


FIG. 2. The $^{28}\text{Si}(^{15}\text{N}, ^{16}\text{O})^{27}\text{Al}$ proton-pickup reaction to the $\frac{5}{2}^+$ ground state and $\frac{1}{2}^+$ 0.84 MeV excited states in ^{27}Al . The theoretical predictions are those obtained using the OMP's (dashed line) and ST potentials (solid line) from Tables I and II. Similar results to those with OMP result from use of folding optical potentials. The relative normalization of the surface transparent and strong absorption results is that predicted by DWBA indicating a strong preference for potentials ST.

these channels is especially sensitive to the value of the surface absorption W_s in each channel. Since this surface absorption is also strongly related to the open direct channels in a particular system, we expect W_s for $^{16}\text{O} + ^{27}\text{Al}$, $^{14}\text{N} + ^{29}\text{Si}$, or $^{15}\text{N} + ^{28}\text{Si}$ to be somewhat greater than for the $^{16}\text{O} + ^{28}\text{Si}$ system. For the moment, with a rather obvious bias in mind, we have selected W_s for the latter three channels to be 1.5, 5.0, and 3.0 M MeV, respectively. Such choices are consistent with the elastic data; $W_s \geq 3.0$ is necessary for the $^{15}\text{N} + ^{28}\text{Si}$ fit up to $\theta_{c.m.} \approx 90^\circ$ while the ^{14}N channel is much less sensitive to this surface absorption. This very interesting backward angle behavior will be returned to later.

For the moment, we return to the proton-pickup and neutron-stripping reactions considered in Ref. 1, with only reactions to what are considered as strong single particle states treated. The predictions for these reactions are shown as angular distributions in Figs. 2 and 3 and as absolute magnitudes for a selective angle in Table III. The cal-

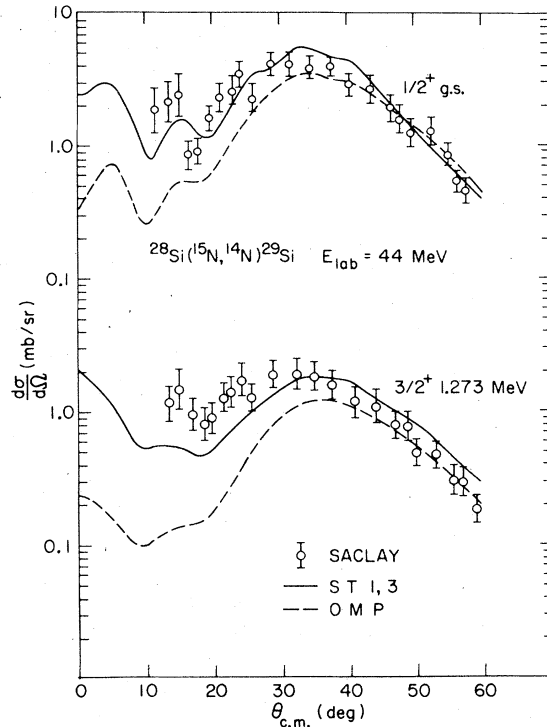


FIG. 3. The $^{28}\text{Si}(^{15}\text{N}, ^{14}\text{N})^{29}\text{Si}$ neutron-stripping reaction to the $\frac{1}{2}^+$ ground state and $\frac{3}{2}^+$ 1.27 MeV excited states. See caption to Fig. 2.

culations using ST potentials from Table II are shown as solid lines and OMP from Table I (strongly absorbing) as dashed lines. The relative normalization between dashed and solid lines is the correct relative normalization arising from DWBA codes. In the present work the DWBA code PTOLEMY of Macfarlane and Peiper⁷ was used for both elastic and transfer calculations. The calculated results differ somewhat from those obtained in Ref. 1 using MARS-SATURN,⁸ as operative at Saclay. The major improvement in the description of the data is evident for the proton-pickup reactions and the more minor improvements required at forward angles for the neutron stripping are also clear. The large related and required increase in transition strength for the ($^{15}\text{N}, ^{16}\text{O}$) reaction is further strong evidence for the necessity of surface transparency.

One expects as in Ref. 1 that the introduction of channel coupling to low lying excited states of the target or projectile will be important only in details of the theoretical calculations for transitions to strong, single particle states. Such channel coupling is, however, often crucial for transitions to more complicated final states which show up as weaker transitions in the measured spectra, and probably in the details of elastic scattering.

TABLE III. Absolute magnitudes of transfer cross sections; spectroscopic factors. The target spectroscopic factors are labeled S2 with a projectile spectroscopic factor S1=2.0 appropriate both for neutron stripping and proton pickup. Cross-section magnitudes are shown at a forward and a near grazing angle to clarify the comparisons when a bell-shaped angular distribution is not appropriate. S2 is extracted for the strong absorption potentials OMP without regard to renormalization of the ground state value, i.e., directly from Figs. 2, 3. For the oscillating, forward rising pickup differential cross sections S1 (OMP) is not meaningful, while S2 (ST) is a rough estimate obtained by averaging over several forward angles. For stripping, S2 is extracted at grazing angles. For the pickup reaction the surface-transparent volume-opaque potentials do a considerably better job of describing absolute magnitudes.

State	Stripping $^{15}\text{N} + ^{28}\text{Si} \rightarrow ^{14}\text{N} + ^{28}\text{Si}$					
	S2			σ (15°) mb/sr		
	ST	OMP	(<i>dp</i>)	EXP	ST	OMP
g.s. $\frac{1}{2}^+$	0.50	0.57	0.53	2.4 ± 0.7	1.60	0.55
1.27 MeV $\frac{3}{2}^+$	0.71	1.07	0.74	1.4 ± 0.5	0.55	0.14

State	Pickup $^{15}\text{N} + ^{28}\text{Si} \rightarrow ^{16}\text{O} + ^{27}\text{Al}$							
	S2				σ (11°) mb/sr			
	ST	(<i>d</i> , ^3He)	EXP	ST	OMP	EXP	ST	OMP
g.s. $\frac{5}{2}^+$	3.05	3.80	10.0 ± 2.0	11.4	0.5	3.8	4.0	1.8
				σ (6°) mb/sr			σ (39°)	
0.84 MeV $\frac{3}{2}^+$	0.60	0.49	7 ± 1.5	6.0	0.3	0.95	1.1	1.1

III. BACKWARD ANGLE SCATTERING

It is clear from the above considerations that any optical potential attempts to explain the very interesting backward angle phenomenon in $^{16}\text{O} + ^{28}\text{Si}$ elastic and inelastic scattering, between center of mass energies $E_{c.m.} = 20$ MeV and $E_{c.m.} = 50$ MeV, must also be applied to transfer reactions. All quasielastic processes in heavy-ion induced reactions must be treated together and thus the transfer reactions even at forward angles provide an extremely important constraint. This point is made more clear by the observation that both backward elastic scattering and forward transfer can be sensitive to distances of approach, for colliding ions, somewhat less than the grazing distance. In optical potential terms these reactions sense the inner spatial regions of the real optical potential, regions just outside of the point where more violent deep inelastic and fusion reactions become important. A fairly evident mistake to make would be to use an optical potential with a rather shallow volume absorption. Such a potential used in DWBA or CCBA might succeed in describing well matched single particle exchange but, in particular, would have great difficulties in predicting badly matched transfer or multinucleon transfer.

Finally, then, it is of interest to test out the

potentials of Table II in predictions of backward angle elastic scattering for the $^{16}\text{O} + ^{28}\text{Si}$ channels. Since these potentials were determined in fits to forward angle scattering in $^{16}\text{O} + ^{27}\text{Al}$ and $^{15}\text{N} + ^{28}\text{Si}$ channels, one cannot expect detailed fits to be made for the complex $^{16}\text{O} + ^{28}\text{Si}$ scattering. In any case, this latter elastic scattering is quite sensitive to coupling to low lying states in ^{28}Si .⁴ In our opinion, a more interesting test is to examine the $(\sigma_{\text{elastic}}/\sigma_{\text{RUTH}})$ (180°) excitation function, since the behavior of this quantity as a function of $E_{c.m.}$ is likely to be more characteristic of the backward angle "glory" phenomenon and is also more likely to persist through the refinements of channel coupling. In Fig. 4, then, we show the results of calculation of the quantity $(\sigma_{\text{el}}/\sigma_{\text{RUTH}})$ (180°) using a potential generally independent of energy variation in the optical parameters aside from an expected, minor alteration in the surface absorption. To move from the elastic channels discussed in this work to the $^{16}\text{O} + ^{28}\text{Si}$ channel, we have altered (aside from $A^{1/3}$ changes) only the surface absorption strength W_s , reducing this quantity to values $W_s \leq 0.5$ MeV in a fashion consistent with the previously expressed philosophy. The rather striking agreement in phase and depth of oscillation in theoretical and experimental³ excitation functions without the introduction of l -dependent artifices⁹ is perhaps an encouraging sign.

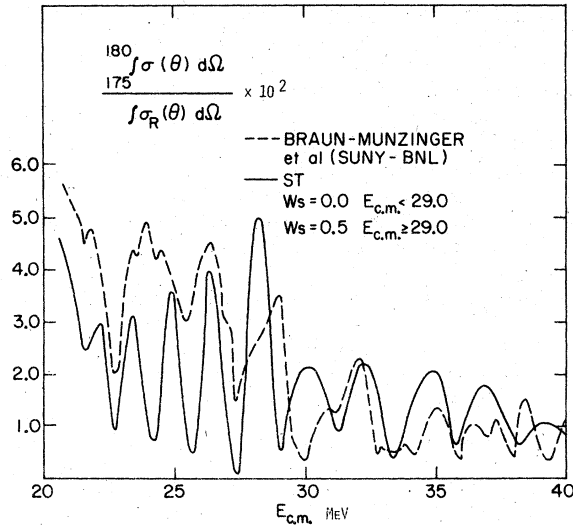


FIG. 4. Elastic excitation function for $(\sigma_{\text{elastic}}/\sigma_{\text{Rutherford}})$ (180°) in units of 10^{-2} . The data (dashed line), sketched in roughly, are from Ref. 3 and other private communications from the same authors. The solid line is the calculation using the potential ST 2 for $^{16}\text{O} + ^{27}\text{Al}$ in the present work. The surface absorption W_s has been reduced to 0.5 MeV for $E_{\text{c.m.}} \geq 29$ MeV and to 0.0 MeV for $E_{\text{c.m.}} < 29$ MeV.

This success in describing the excitation function for $^{16}\text{O} + ^{28}\text{Si}$ back angle scattering should be somewhat tempered by the realization that detailed fits to elastic scattering angular distribution at each energy may still be difficult. Nevertheless, it would appear that further investigation of the gross energy structure in the backward angle phenomenon with the use of optical potentials is likely to be quite fruitful.

The specific nature of the real potential is clearly important. The real potentials in Tables I or II both yield pockets, albeit shallow, which suggest the presence of a collaborative resonantlike phenomenon in several of the grazing partial waves. The success in describing the excitation function can be attributed to the specific balance between geometry and depth in the real potential, combining to keep the correct partial waves near enough to their respective barriers. This point will be examined in greater detail in a more extensive work.

IV. SUMMARY AND CONCLUSIONS

The main objective of this paper, to improve the theoretical treatment of single nucleon pickup and stripping reactions induced by a ^{15}N projectile on a ^{28}Si target has clearly been achieved. The introduction of volume-opaque, surface-transparent

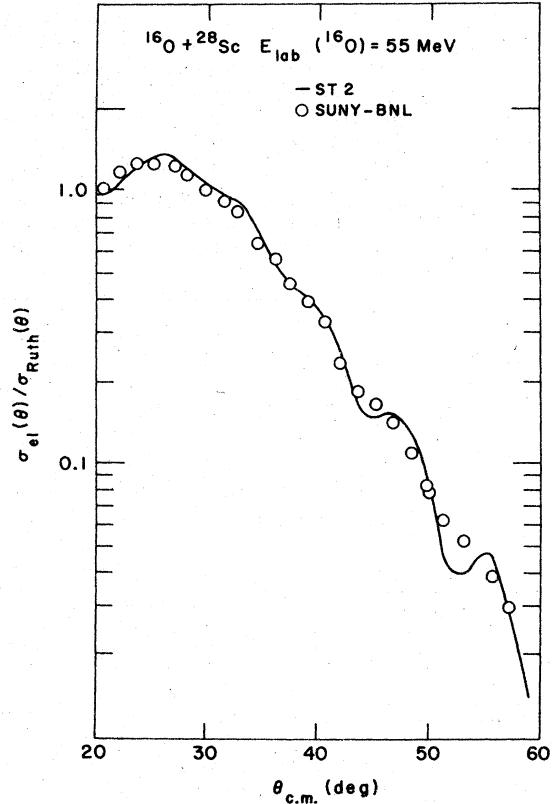


FIG. 5. Forward angular distribution for $E_{\text{c.m.}} = 35$ MeV, $^{16}\text{O} + ^{28}\text{Si}$ scattering using the ST 2 potential with $W_s = 1.0$ MeV. ST 2 was of course fitted to $^{16}\text{O} + ^{27}\text{Al}$; nevertheless, the description of the neighboring channel is quite good. No experimental errors are indicated in this illustrative calculation.

absorptive potentials produces theoretical reaction cross sections, both in shape and magnitude, in excellent agreement with experiment. The theoretical description of elastic scattering for center of mass angles $\theta \leq 80^\circ$ is preserved by reasonable choices for the level of surface absorption W_s . A general consistency then results between the backward angle behavior observed in the neighboring system $^{16}\text{O} + ^{28}\text{Si}$ and the forward angle transfer reactions induced by ^{15}N . It should be noted that the increase in W_s from the range 0–0.5 MeV in $^{16}\text{O} + ^{28}\text{Si}$ to 1.5–5.0 MeV in the $^{16}\text{N} + ^{27}\text{Al}$, $^{15}\text{N} + ^{28}\text{Si}$, and $^{14}\text{N} + ^{29}\text{Si}$ systems is sufficient to greatly reduce the magnitude of the backward rise in $(\sigma_{\text{el}}/\sigma_{\text{RUTH}})$ ($\theta_{\text{c.m.}}$), although not sufficient to eliminate this phenomenon. One's picture of the nuclear structure of ^{16}O , ^{28}Si ties in nicely with a reduced value of surface absorption.

It appears from existing data that the resonantlike phenomena seen in backward elastic inelastic and forward transfer excitation functions is strongest when target and projectile have a clear, $A = 4N$,

α structure. Adding a few valence nucleons to the projectile or target probably does not alter the real ion-ion potential appreciably, but does increase the direct reaction contribution to absorption thus leading to an increase in W_s . As seen above, a rather small increase in W_s is sufficient to greatly reduce the magnitude of any structure in excitation functions.

It has not been demonstrated here that the potentials of Table II when applied to elastic scattering will yield detailed predictions for the angular distribution at varying bombarding energies, i.e. for center of mass energies just above the Coulomb barrier to perhaps $2\frac{1}{2}$ times the barrier. Nevertheless, it is clear that the pickup and stripping reactions will not be well described by a model which fails to account, at least qualitatively, for the backward angle elastic scattering. The potentials ST yield an optical model description of the backward phenomenon which encompasses both elastic and inelastic events. The elastic S matrix for these potentials will be described in a future work which will examine more carefully angular distributions at all energies, especially at the lower energies near the barrier.

As a slight caveat we again refer to detailed elastic scattering in the sensitive $^{16}\text{O} + ^{28}\text{Si}$ channel. The choice of W_s values for the excitation function in Fig. 4 was of course meant to be illustrative. It is absolutely clear that low values of surface are required to produce the needed transparency

in this channel, but it is also clear that some smoother variation of W_s is required. Indeed, examination of Fig. 4 suggests that a somewhat higher value is needed for $E \geq 30$ MeV. It is rather gratifying then that when a value $W_s = 1.0$ MeV is used with the potential ST 2 the well studied $E_{c.m.} = 35$ MeV forward angle $^{16}\text{O} + ^{28}\text{Si}$ (Ref. 3) scattering (Fig. 5) is perhaps better described than in many earlier studies specifically fitted to this channel, while the excitation function for the higher center of mass energies is unaltered in shape but lowered somewhat in magnitude. The forward angle scattering is, of course, not overly sensitive to W_s , but more care is to be taken in backward hemisphere scattering. More extensive elastic studies are now being pursued at the lowest energies in Fig. 4 and verify that very small values of W_s are essential.

ACKNOWLEDGMENTS

One of the authors, S. H. Kahana, is grateful to the Department de Physique Nucleaire, CEN, Saclay, France for support and hospitality while he was at Saclay and to S. Pieper, Argonne National Laboratory, for rendering the program PTOLEMY operational at Brookhaven National Laboratory. This work was partially supported by U. S. Department of Energy under Contract No. EX-76-C-02-0016.

¹J. C. Peng, B. T. Kim, M. C. Mermaz, A. Greiner, and N. Lisbona, Phys. Rev. C **18**, 2179 (1978).

²A. J. Baltz, P. D. Bond, J. D. Garrett, and S. H. Kahana, Phys. Rev. C **12**, 136 (1975).

³P. Braun-Munzinger, G. M. Berkowitz, T. M. Cormier, C. M. Jachcinski, J. W. Harriss, J. Barrette, and M. J. LeVine, Phys. Rev. Lett. **38**, 944 (1977).

⁴S. H. Kahana, Proceedings of the Symposium on Heavy-Ion Elastic Scattering, University of Rochester, 1977 (unpublished).

⁵D. Dehnhard, Proceedings of the Symposium on Heavy-Ion Elastic Scattering, University of Rochester, 1977

(unpublished).

⁶R. DeVries, Proceedings of the Symposium on Heavy-Ion Elastic Scattering, University of Rochester, 1977 (unpublished).

⁷M. H. Macfarlane and Steven C. Pieper, Argonne National Laboratory Report No. ANL-76-11, Rev. 1, Argonne, Illinois, 1976.

⁸T. Tamura, T. Udagawa, and B. T. Kim, unpublished.

⁹D. Dehnhard, V. Shkolnik, and M. A. Franey, Phys. Rev. Lett. **40**, 1549 (1978).

¹⁰M. C. Mermaz, M. A. G. Fernandes, A. Greiner, B. T. Kim, and N. Lisbona, Phys. Rev. C **19**, 794 (1979).